Astron. Astrophys. 364, 723–731 (2000)

ASTRONOMY AND ASTROPHYSICS

Extended red emission and unidentified infrared bands in the galactic compact H II region Sh 152⋆

S. Darbon[1], **A. Zavagno**[2], **J.-M. Perrin**[1], **C. Savine**[1], **V. Ducci**[2], **and J.-P. Sivan**[1]

[1] Observatoire de Haute Provence du CNRS, 04870 Saint Michel l'Observatoire, France
[2] Observatoire de Marseille, 2 Place Le Verrier, 13248 Marseille Cedex 4, France

Received 22 November 1999 / Accepted 28 September 2000

Abstract. We present visible and infrared images and low-dispersion visible spectra of the galactic compact H II region Sh 152. The spatial distribution of the Extended Red Emission (ERE) over the nebula is found to coincide with that of the ionized hydrogen emission and to differ from that of the Unidentified InfraRed Bands (UIRBs) emission at 3.3 and 6.2 μm. This result and other considerations are in favour of grains as carriers of the ERE. It is shown that nanosized silicon particles could account for the ERE in terms of luminescence, an interpretation which, however, suffers from some limitations.

Key words: scattering – ISM: individual objects: Sh 138 – ISM: dust, extinction – ISM: H II regions – infrared: ISM: lines and bands

1. Introduction

The Extended Red Emission (ERE) is a continuous emission band generally observed in the red part (600–800 nm) of the spectrum of various dusty astrophysical objects: reflection nebulae (Schmidt et al. 1980; Witt & Boroson 1990), planetary nebulae (Furton & Witt 1992), galactic and extragalactic H II regions (Perrin & Sivan 1992; Sivan & Perrin 1993; Darbon et al. 1998), high-latitude galactic cirrus clouds (Szomoru & Guhathakurta 1998), the halo of the galaxy M82 (Perrin et al. 1995) and the diffuse galactic medium (Gordon et al. 1998). It has been commonly explained by luminescence from Quenched Carbonaceous Composites (f-QCC) (Sakata et al. 1992), Hydrogenated Amorphous Carbon (HAC) grains (see for example Furton & Witt 1993; Seahra & Duley 1999), silicon nanocrystals (Witt et al. 1998; Ledoux et al. 1998) or from isolated molecules such as free Polycyclic Aromatic Hydrocarbon (PAH) molecules (see for example d'Hendecourt et al. 1986; Léger et al. 1988). Emission bands in the 3–16 μm range, the so-called Unidentified InfraRed Bands (UIRBs), are also observed in dusty environments (e.g. Sellgren 1981) and commonly attributed to PAH molecules (see for example Puget & Léger 1989; Allamandola et al. 1989) and/or carbonaceous materials (see for example Papoular et al. 1989). The existence (or absence) of a spatial correlation between UIRBs and ERE might be useful to put constraints on the nature of the carriers.

Compact H II regions, which are bright and dusty objects, seemed to us well suited for this kind of study. We therefore carried out a program of imagery and spectrophotometry of compact H II regions in order to detect and map ERE and UIRBs. This paper reports on the results obtained for Sh 152, a compact H II region, previously known as an intense near-IR source (Frogel & Persson 1972). Among the three main stars present in this object (see Fig. 2 in Heydari-Malayeri & Testor 1981), only the component S 152.1, of spectral type O9V (Hunter & Massey 1990), plays a role in the ionization and excitation of the nebula. An ionization front is clearly visible at the south and the east of S 152.1 and is closely associated with dust (Heydari-Malayeri & Testor 1981; Cox, Deharveng & Caplan 1987).

Sect. 2 describes the observations and data reduction. Sect. 3 presents the spatial correlation between visible and IR emissions. Sect. 4 shows the main spectrophotometric results we have interpreted in terms of dust scattering and luminescence. Discussion and conclusions are given in Sect. 5.

2. Observations and data reduction

Infrared images of Sh 152 were obtained with ISOCAM in June 1997, during ISO revolution 563. These include UIRBs images at 3.3 and 6.2 μm and four continuum images taken with the ISOCAM circular variable filter (CVF) at 6.911, 8.222, 10.52 and 12.00 μm. These observations and data reduction are described in details by Zavagno & Ducci (1999).

Visible images in the 500-850 nm range were obtained in October 1997 with a 1024 $\times$ 1024 thinned back-illuminated Tektronix CCD camera mounted at the Newton focus of the 120 cm telescope of the Observatoire de Haute Provence. Four interference filters, 10 nm wide (FWHM), centered on 528.2, 612.0, 697.5 and 812.5 nm were used to sample the continuum emission of Sh 152, avoiding nebular and night sky emission lines (Fig. 2). For each continuum filter, twenty-four 15 min exposure frames were obtained and co-added, yielding a resulting

Send offprint requests to: J.-P. Sivan

⋆ Partly based on observations made at Observatoire de Haute Provence du CNRS (France) and with ISO, an ESA project with instruments funded by ESA Member States (especially the PI countries: France, Germany, the Netherlands and the United Kingdom) and with the participation of ISAS and NASA.

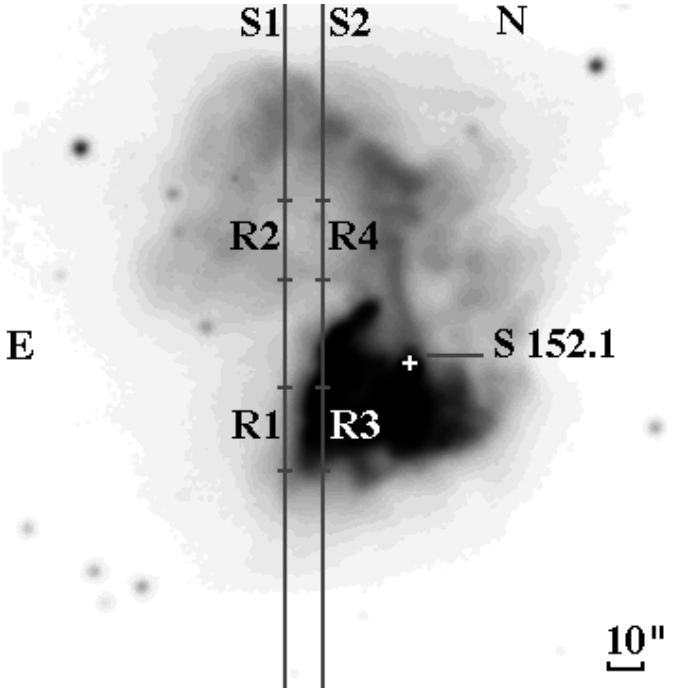

Fig. 1. Spectrophotometric observations of Sh 152: the spectrograph slit positions S1 and S2 (respectively at $30''$ and $20''$ east of the exciting star S 152.1) are drawn on an Hα image of the nebula (taken at Observatoire de Haute Provence). Windows over which one-dimensional spectra were extracted are labelled R1 to R4.

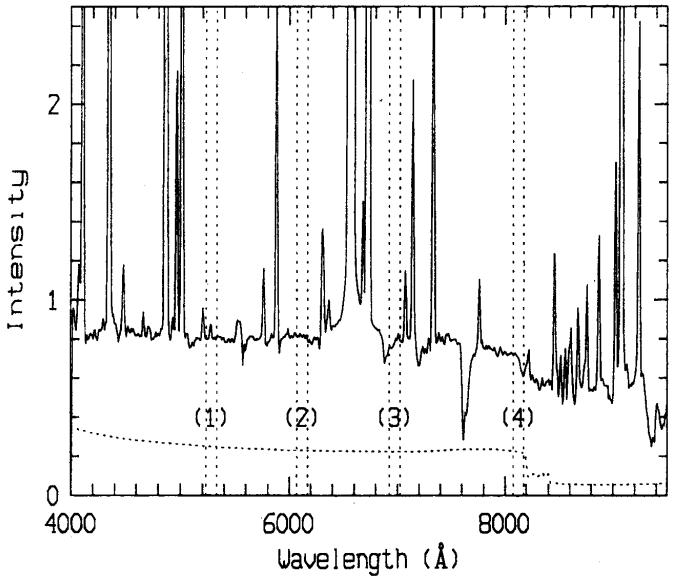

Fig. 2. Dereddened spectrum of region 1 of Sh 152; the theoretical atomic continuum spectrum is superimposed in dotted line (intensity in 10^{-6} erg cm^{-2}s^{-1}Å^{-1}sr^{-1}). Vertical dotted lines indicate the band-passes (1) to (4) of the filters used for narrow-band imaging of Sh 152.

Table 1. Position and dimensions of regions observed over Sh 152

	Region Center[a]			
Region	$\Delta\alpha$	$\Delta\delta$	Dimension	Position Angle
1.....	$30''$ E	$15''$ S	$22''.2 \times 3''.0$	$00°$
2.....	$30''$ E	$27''$ N	$16''.4 \times 3''.0$	$00°$
3.....	$20''$ E	$15''$ S	$24''.6 \times 3''.0$	$00°$
4.....	$20''$ E	$27''$ N	$21''.1 \times 3''.0$	$00°$

[a] Offset angles are relative to the exciting star

image of six hours exposure time. Data reduction is described in detail by Darbon et al. (1999a). The nebula ERE map is obtained by subtracting the 612.0 nm image from the 697.5 nm one.

Spectra of Sh 152 were obtained in October 1996 and October 1997 at the Cassegrain focus of the 193 cm telescope of the Observatoire de Haute Provence using the Carelec long-slit spectrograph (Lemaître et al. 1990) equipped with a thinned back-illuminated Tektronix CCD. The spectral domain 4000-9600 Å was covered with a dispersion of 277 Å mm^{-1}. The slit width was $3''.0$, which corresponds to a resolution of 21.6 Å. Two north-south slit positions were observed on the nebula, located respectively $30''$ and $20''$ east of the exciting star (Fig. 1).

600 s elementary exposures were obtained, keeping the nebula alternatively in the northern or the southern half of the spectrograph slit. This allowed us to observe simultaneously the nebula and the surrounding sky background. By taking an even number of such short exposures, we could subtract (after offset subtracting and flat-fielding) from the nebula spectrum the sky background spectrum observed exactly at the same pixels as the nebula, thus avoiding any instrumental effect. Total exposure times of 8400 s and 12000 s were obtained for slit positions 1 and 2 respectively. A short (600 s) exposure was obtained for a north-south slit position centered on the exciting star.

Each nebula spectrum was spatially divided into two regions free of contamination by stellar spectra (Fig. 1 and Table 1): regions 1 and 3 are located on the component A of the nebula (respectively behind and on the ionization front) whereas regions 2 and 4 are on the component B (Heydari-Malayeri & Testor 1981). One-dimensional spectra were extracted for each region, calibrated and corrected for atmospheric extinction. The same procedure was applied to the spectrum of the exciting star. The spectra were corrected for foreground interstellar extinction using the standard galactic extinction curve as previously described (Sivan & Perrin 1993) and using $E_{B-V} = 0.45$ (Nandy et al. 1976).

Also, as explained in Sivan & Perrin (1993), we calculated for each region the continuous emission arising from the nebula atomic gas assuming a pure hydrogen nebula (i.e. neglecting He contribution) and using the electron temperature and density derived from N II and S II line intensity ratios (Table 2). The calculated atomic spectra were subtracted from the dereddened nebula spectra (Fig. 2).

It should be noted that this subtraction allows us to validate a posteriori the value of the reddening we have used. A variation as small as 10% in E_{B-V} modifies the temperature in such a manner that the amplitude of the theoretical Paschen jump no longer matches the observations.

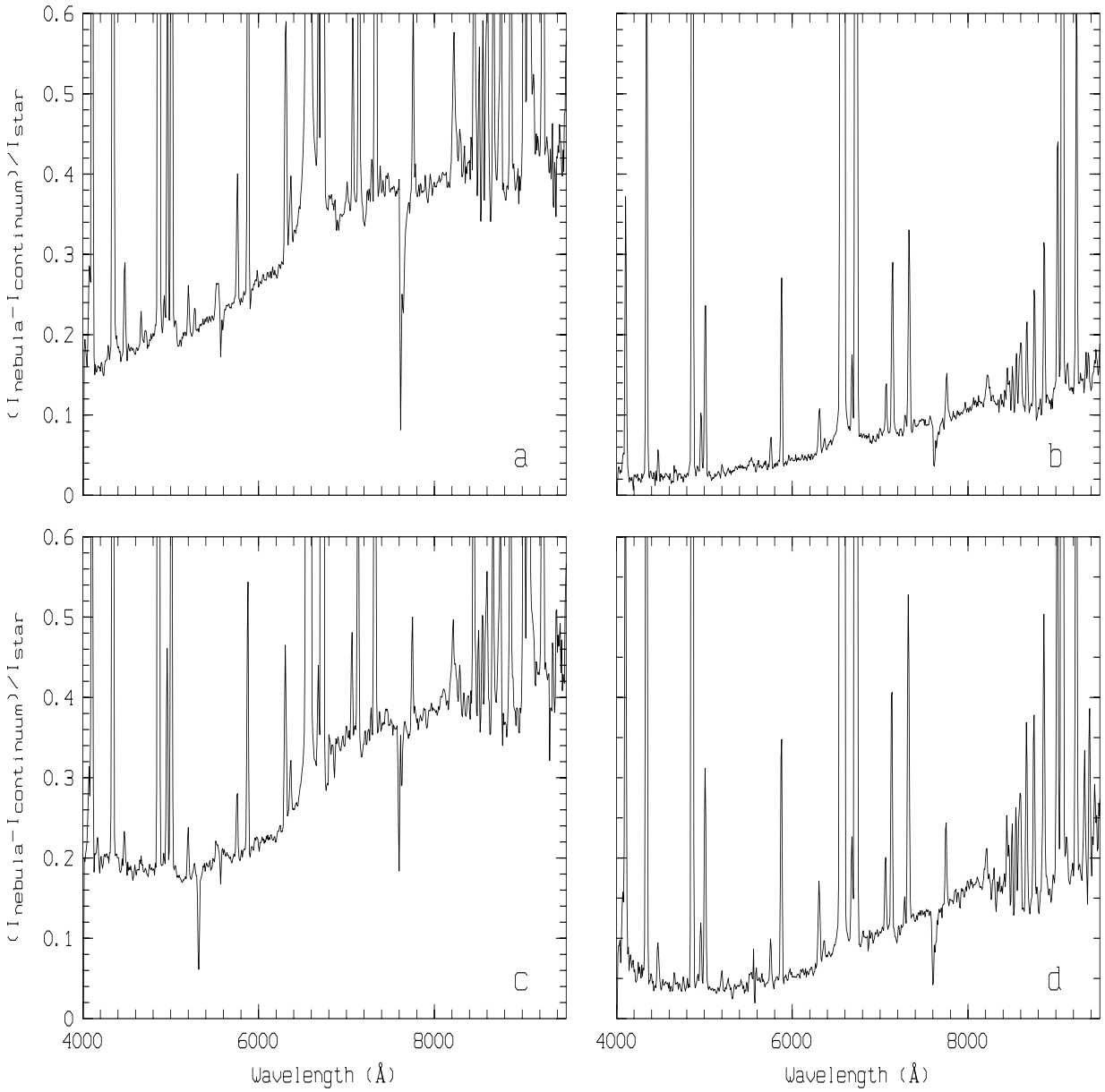

Fig. 3a–d. Division of the nebula spectra corrected for atomic continuum emission by the spectrum of the exciting star, for regions 1 (**a**), 2 (**b**), 3 (**c**) and 4 (**d**) (see Fig. 1)

To characterize the scattering and, eventually, the luminescence phenomena, we have divided the dereddened spectrum of each region, corrected for atomic continuum emission, by the dereddened spectrum of the exciting star. The results are shown in Fig. 3. This assumes the same nebular structure as Heydari-Malayeri & Testor (1981): the star S 152.1 is embedded in a quite homogeneous cocoon of dust and gas (Cox, Deharveng & Caplan 1987) so that its spectral energy distribution is the same in the direction of the observer as well as in the direction of regions 1 to 4 in the nebula. Finally, in order to obtain the spectral characteristics of the ERE, the contribution of the scattering was subtracted from these spectra. This contribution was calculated from models of cosmic dust using size distribution laws of grains made with materials of astrophysical interest (see Sect. 4).

Table 2. Electron temperatures and densities

Region	T_e (K)	n_e (cm^{-3})
1.....	8000	400
2.....	7500	1000
3.....	10900	1000
4.....	9200	1000

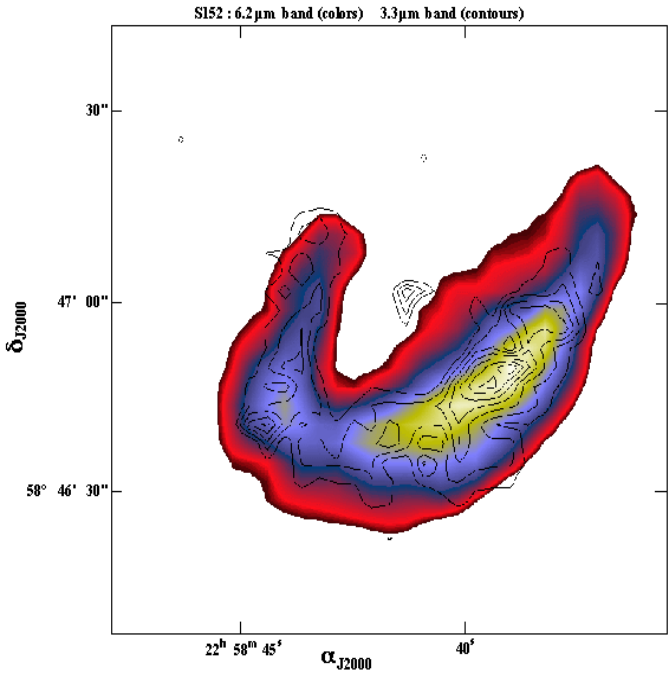

Fig. 4. 6.2 μm (colors) and 3.3 μm (solid contours) emission bands in Sh 152

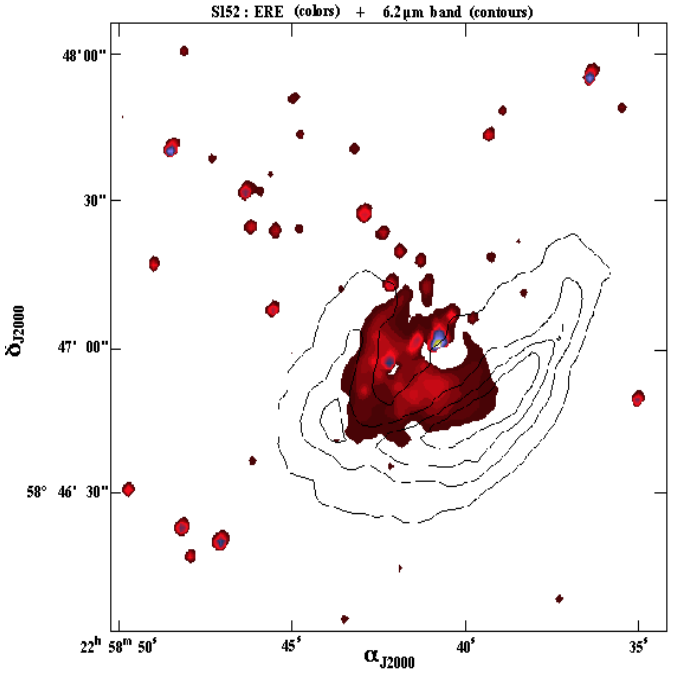

Fig. 6. ERE distribution (colors) and 6.2 μm emission (solid contours) in Sh 152

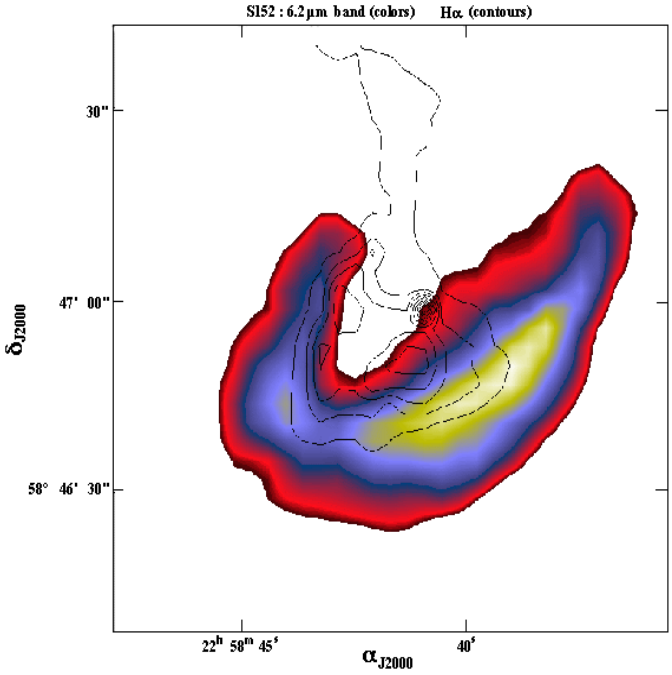

Fig. 5. 6.2 μm emission band (colors) and Hα emission (solid contours) in Sh 152

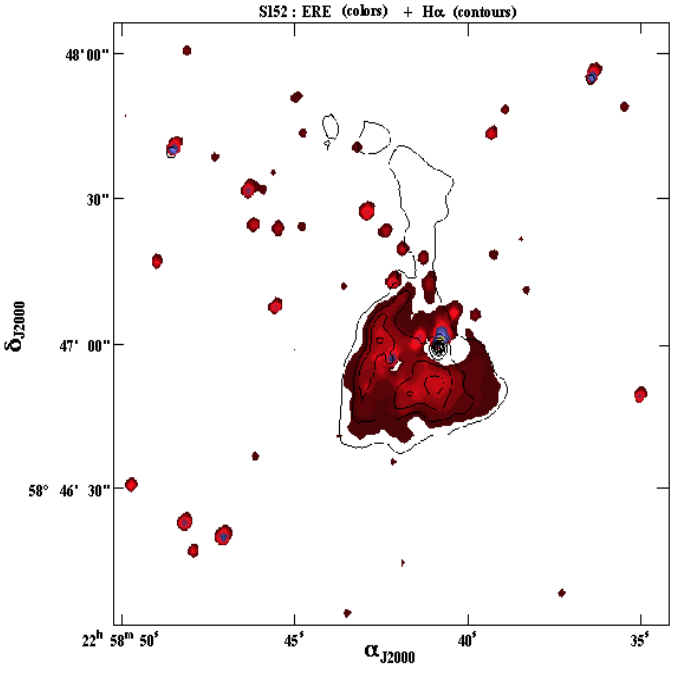

Fig. 7. ERE distribution (colors) and Hα emission (solid contours) in Sh 152

3. Imagery results

Figs. 4 to 8 allow intercomparisons of the spatial distribution of several infrared and visible emissions over Sh 152, namely those arising from the 3.3 and 6.2 μm UIRBs, the 12 μm continuum, the Hα line and the ERE. The main results shown by these figures can be summarized as follows.

The 3.3 and 6.2 μm emission bands have the same spatial distribution over the entire nebula, suggesting that their carriers could be the same. The maxima of the infrared emissions arise from regions located outside the ionized region (traced by Hα emission) but the ERE contours are found to closely coincide with those of the ionized region and thus significantly differ from the UIRBs distribution. This anti-correlated spatial distri-

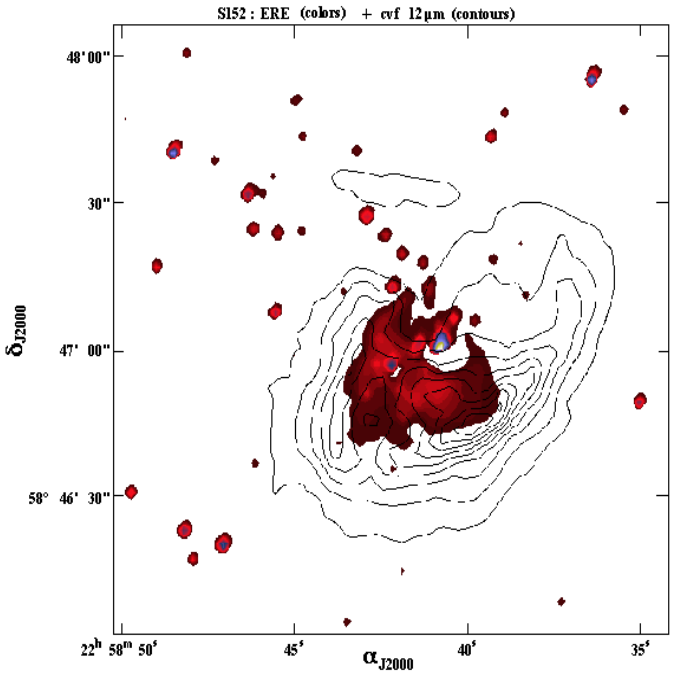

Fig. 8. ERE distribution (colors) and 12 μm continuum emission (solid contours) in Sh 152

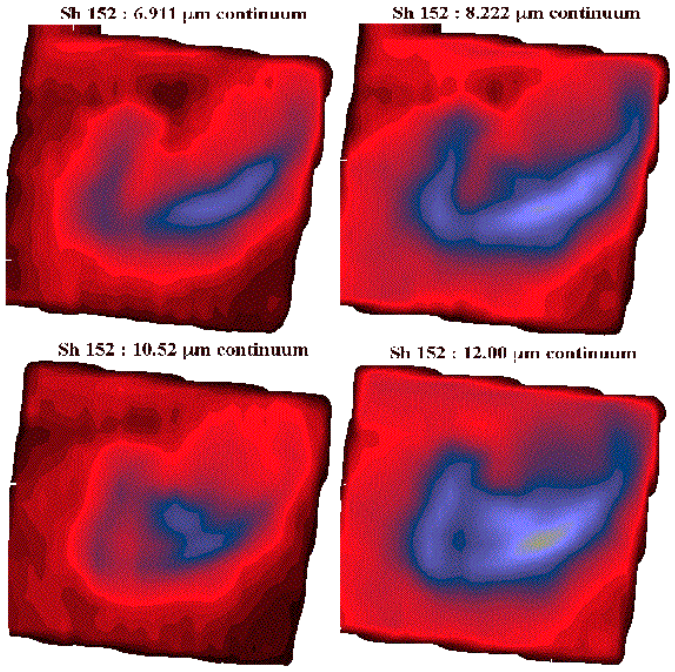

Fig. 9. Continuum emission in Sh 152 observed with the ISOCAM CVF at 6.911, 8.222, 10.52 and 12.00 μm

bution of ERE and UIRBs is very similar to the results of Kerr et al. (1999) for the Red Rectangle nebula. Also, the 12 μm continuum emission extends over the area where the ERE intensity reaches its maximum. This coincidence is in favour of grains as carriers of the ERE (i) because the 12 μm emission is thought to be the short wavelength part of a strong thermal emission from grains (see, for example, IR spectra of ultra compact galactic H II regions presented by Roelfsema et al. 1998) and (ii) because such grains can exist in Sh 152 at the distance from the exciting star where the observed coincidence occurs. In effect, this area is located about 0.2 pc from the star (assuming a distance of 3.5 kpc for Sh 152, Heydari-Malayeri & Testor 1981). According to Lamy & Perrin (1997), the temperature of a dust particule located between 10^{-3} pc and 0.2 pc from an O9.5V star would be lower than 200 K for a silicate grain and 400K for a carbonaceous grain.

Fig. 9 presents the four continuum images of Sh 152 at 6.911, 8.222, 10.52 and 12.00 μm taken with ISOCAM. In these images, the flux is normalized to the maximum observed in the LW6 filter, centered at 7.7 μm. At the location of the ERE maximum, the infrared images show flux values increasing with wavelength: this is in agreement with thermal emission from grains. It should be noted that the ionizing potential of OIII and SIV are about the same ($\simeq$ 35eV) and that, since the [OIII]λ5007Å emission is extremely weak (Fig. 4b of Heydari-Malayeri & Testor 1981) at the location of the maximum of the 10.52 μm emission, the ISOCAM 10.52 μm image is unlikely to be contaminated by the [SIV] 10.521 μm emission line.

4. Spectrophotometric results

The spectra in Fig. 3 exhibit a continuum which, as a mean, dramatically increases from 4000 to 9500 Å. One possible explanation could be that the optical depth of the dust surrounding the star Sh 152.1 is larger in the direction toward the four studied regions than toward the observer (Witt 1985). However, the 12 μm continuous emission maps in Figs. 8 & 9 suggest that the dust density is smaller between the star and region 4 than between the star and region 1. The two regions are at the same distance from the star and the mean gradient in region 4 is much more larger than the gradient in region 1 (Fig. 3). As a result, the above explanation does not seem to be valid and the physical properties of the grains should be invoked to explain why the nebula appears to be much redder than the star.

Consequently, we have tried to fit the observed continuous spectra of Sh152 (Fig. 3) by scattering calculations using several grain size distributions, several scattering angle intervals and several materials of astrophysical interest. We have used only simple scattering since the nebula optical depth is small outside the star cocoon. Also, we retained only the model scattering spectra that (i) fit the observed spectra at least in their bluest ($\lambda \leq 5500$Å) and reddest ($\lambda \geq 9000$Å) parts and (ii) undergo only very small changes when scattering parameters are slightly modified (stationary solution).

Scattering spectra of classical H II regions, which exhibit negative or barely positive gradients, are explained by stellar light scattered by HAC grains (Sivan & Perrin 1993). The same explanation could be applied to Sh 152, assuming a larger proportion of HAC grains with a size parameter greater than 1. Such large grains can exist in the vicinity of an O9 (or later-type) star according to Lamy & Perrin (1997): the radiative pressure acting on the smallest grains being greater than the gravitational attrac-

Table 3. Parameters of the scattering models fitting the observed spectra of Sh 152

	Radius Size Range (μm)		Scattering	p (Exponent of
Region	core	grain	angle interval	size distribution)[1]
1.....	0.003,0.6	0.005,1.0	$[15°, 30°]$	0.75
3.....	0.001,0.1	0.01,1.0	$[15°, 30°]$	0.75

[1] the number of grains with a given radius a is proportional to a^{-p}

tion, these grains are expelled far from the star, thus leading to an increase in the relative abundance of micron-sized grains.

The scattering spectra calculated with HAC grains failed to fit the observations. Same negative results were obtained for various other carbonaceous materials: tholins, icetholin, kerogen, poly-HCN, glassy carbon, amorphous carbons, graphite. We tried to model the scattering component using a number of other materials: silicates (olivine, andesite, augite,...), metals (iron, nickel), iron sulphides (pyrrhotite, troilite), silicon carbides and meteoritic materials. Homogeneous grains, coated grains and solid particles with inclusions were tested. We also considered several grain size distributions in the line of sight. *Only grains composed of silicon-based elements were found to fit the observations satisfactorily*. This result is in agreement with the recent detection of interstellar grains in the solar system (Landgraf et al. 1999).

The best fit to the scattering component was given for region 1 by a model using grains formed by a core of silicon with a coating of silicon carbide (Fig. 10a) and for region 3 by a model using grains with a silicon core and an obsidian coating (Fig. 10b). For regions 2 and 4, the best fit (Figs. 10e & f) was obtained by using grains composed of olivine with inclusions of silicon (respectively 10% and 5% of the total mass). Note that for region 4 we used two size distributions to fit the scattering satisfactorily in particular below 5000 Å; we cannot exclude, however, that the rising of the spectrum in this spectral domain is due to radioluminescence (Blair & Edgington 1968; Nash 1966; Nash et al. 1975). The parameters of the fit are given in Table 3. The values of the exponent of the size distribution p used in these models, which are lower than those found in the diffuse interstellar medium ($p \simeq 3.5$), are in agreement with the relative abundance of micron-sized grains, as found by Landgraf et al. (1999).

As is apparent from Figs. 10g & h, regions 2 and 4 do not exhibit ERE. On the contrary, for regions 1 and 3, an ERE band is unambiguously detected (Figs. 10c & d). This is in agreement with the ERE map (Fig. 6) derived from our visible continuum images. The ERE band in Sh 152 looks similar to those found in galactic H II regions (Perrin & Sivan 1992; Sivan & Perrin 1993), with a peak wavelength around 7200 Å and a width around 1000 Å as defined by Witt & Boroson (1990). The ratio of integrated ERE intensity in the 6000-9000 Å range to the scattered light intensity is 0.20 ± 0.05 for region 1 and 0.10 ± 0.05 for region 3. These values fall within the average of those found in reflection nebulae (Witt & Boroson 1990).

In recent studies (Perrin et al. 1995; Darbon et al. 1998), we showed that the same grain material, namely carbonaceous material, could account simultaneously for the scattering and the ERE in the observed nebulae. For Sh 152, the question is whether silicates and silicon based materials, found to explain the scattering in the nebula, can also explain the ERE in terms of luminescence. The answer is a priori negative since the bulk materials we have used to model the scattering component of the spectra are known to be poor light emitters. However, porous silicon (see for example Canham 1990) as well as nanosized silicon particles (Ledoux et al. 1998; Witt et al. 1998) can give rise to photoluminescence phenomena several orders of magnitude brighter than those yielded by the bulk material.

Can such porous and/or small particles be included inside grains (or in the size distribution) without modifying the results of the scattering calculations? If we consider the complex index of refraction, it appears that, for nanosized particles, the mean free path of electrons being disturbed by the boundaries, in the visible (i.e. at frequencies much lower than the plasma frequency), the real part of the refractive index decreases with respect to that of the bulk material (Bohren & Huffman 1983). Also, as the size of the particle decreases, the space between lattice planes increases (Hofmeister et al. 1999) and the complex index of refraction decreases. Another indication comes from studies of optical properties of porous silicon: although there is no reliable way to link roughness to scattering by a surface, a model of the reflectance of a rough surface of silicon is obtained using a decrease in the imaginary part of the index (Theiß 1997).

These results are confirmed by measurements of reflectivity on porous silicon whose upper layer consists of a great number of isolated or connected monocrystalites. The complex index of refraction is obtained from the Kramers-Kronig analysis of the reflectance spectrum (Koshida et al. 1993; von Behren et al. 1995). In the visible the real and imaginary parts of the index are found to be much more lower than the value obtained for the bulk crystaline silicon. These results should be valid even if the upper layer is completely amorphous (Noguchi et al. 1992). Then, it appears that the scattering properties of nanosized or porous grains of silicon could be given by "effective indexes" which look, in the visible, like the refractive indexes of silicate (Zubko et al. 1999), thus inducing only small changes in the scattering models.

5. Discussion and conclusion

By comparing visible and infrared images of Sh 152 we have found that:

- the spatial distribution of the two UIRBs at 3.3 and 6.2 μm are the same, suggesting similar properties for their carriers,
- the UIRBs emission peak is located at the border of the ionized region,
- the ERE location coincides with the ionized region and significantly differs from the UIRBs location,
- the continuum emission observed at 10.5 and 12 μm is in favor of grains as carriers of the ERE.

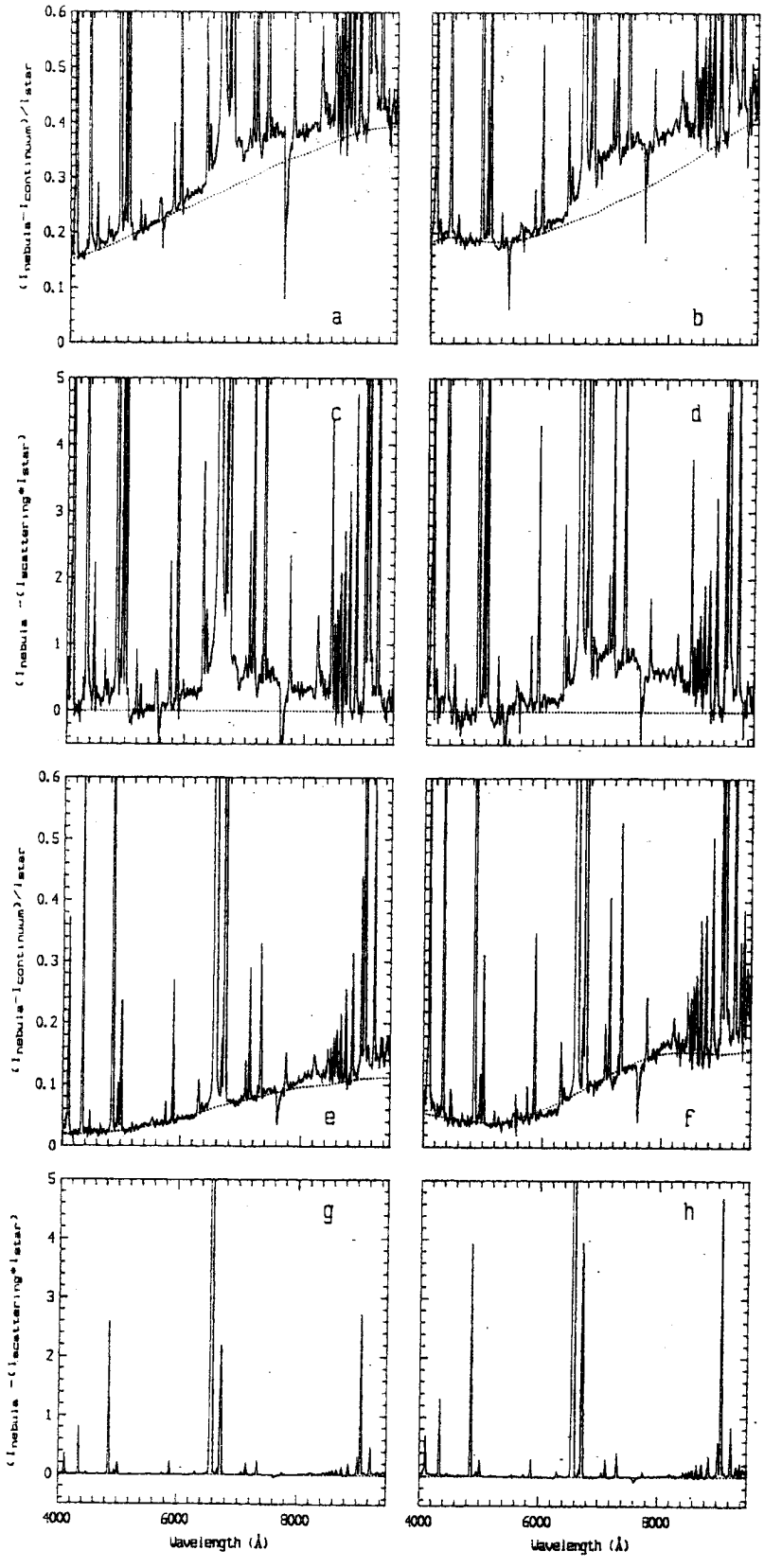

Fig. 10. a, **b**, **e** & **f**: same figures as respectively Figs. 3a,c,b & d. The dotted lines are the model scattering spectra (Table 3) which best fit the observed continuum spectra (after subtraction of atomic continuum and division by stellar spectrum) for regions 1 (**a**), 3 (**b**), 2 (**e**) & 4 (**f**) in Sh 152. **c**, **d**, **g** & **h**: ERE spectral energetic distribution (in 10^{-6} erg cm^{-2} s^{-1} Å^{-1} sr^{-1}) obtained for regions 1 (c), 3 (d), 2 (g) & 4 (h) by subtracting the model scattering spectra multiplied by the exciting star spectrum from the observed nebula spectra corrected for atomic emission.

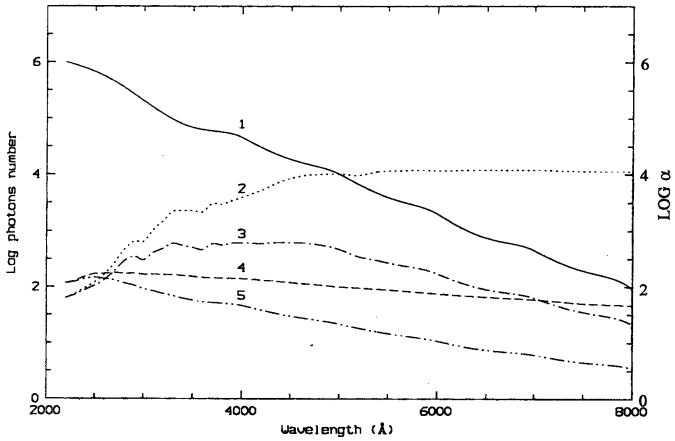

Fig. 11. Variation with wavelength of the number of efficient photons needed to induce ERE in region 1 of Sh 152 (5) and in the reflection nebula VDB 035 (3). These functions are derived from curves (1), (4) and (2) which represent the spectral variations of respectively the absorption coefficient α (cm^{-1}) of nanocrystals of silicon (1) (Ledoux 1999), the flux of photons illuminating region 1 in Sh 152 (4) and the flux of photons illuminating the reflection nebula VDB 035 (2).

From spectrophotometric data, we have found that the scattering spectra of Sh 152 could be explained by grains made up of silicates and silicon and that nanoparticles or porous grains of silicon could account for the observed ERE in terms of photoluminescence.

Laboratory studies have shown that luminescence from porous silicon with amorphous (Noguchi et al. 1992) or crystalline (Koshida et al. 1993) nanostrucures might be explained by electron quantum confinement. The shape of the ERE band and its width and peak wavelength would depend on the size distribution of the nanoparticles (see for example Wilson et al. 1993; Ledoux 1999). Moreover, owing to the high luminescence yield of silicon, the observed ERE intensity is compatible with the cosmic abundance of silicon.

Up to now, no other observational evidence exists for the presence of nanoparticles or highly porous grains of silicon in the interstellar medium. However, laboratory results suggest that different kinds of silicon-based nanoparticles might be present in this medium.

- Nanoparticles of silicon with an oxide shell can be found in micron-sized grains of silicate from non stoechiometric condensation. It has been shown that they can yield luminescence under ultraviolet irradiation (Lu et al. 1995).
- Silica implanted with Si^+ ions can give rise to luminescence phenomena (Kachurin et al. 1997).
- Hydrogen passivated silicon nanoparticles can also yield luminescence (Estes & Moddel 1996a,b); in this case, the bond-stretching, bending and wagging absorption features due to the Si–H bending (see for example Brodsky et al. 1977) should be observed.

If nanosized silicon particles or highly porous grains of silicon are the carriers of the ERE, it should be noted, however, that this interpretation suffers from some limitations. In a recent paper (Darbon et al. 1999b), we have shown that ERE does not occur in nebulae illuminated by stars whose effective temperature is lower than 10000K. Supposing that nanosized crystals of silicon are present in these nebulae as well as in Sh 152, we found (Fig. 11) that the number of efficient photons needed to induce ERE is much smaller for Sh 152 (region 1) than for VDB 035, a reflection nebula where no ERE is detected. This contradiction could be resolved if the materials and/or the size of the particles in the vicinity of stars colder than A0 are not the same as in the vicinity of hotter stars. Moreover, at least up to now, it seems that nanosized particles of silicon have been found neither in meteorites nor in lunar rocks, even when single crystal X-ray diffraction methods are used (see for example Bradley & Brownlee 1991). Such fine laboratory studies on cosmic materials as well as future space missions directed toward comets are likely to yield fundamental data on these particles.

Acknowledgements. We wish to thank the night assistants of Observatoire de Haute Provence for their help during the observations. We are also grateful to C. Reynaud, O. Guillois and G. Ledoux for useful discussions and to the referee, Prof. A. Witt, for helpful comments.

References

Allamandolla L.J., Tielens A.G.G.M., Barker J.R., 1989, ApJS 71, 733
Blair I.M., Edgington J.A., 1968, Nat 217, 157
Bohren C.F., Huffman D.R., 1983, Absorption and Scattering of Light by Small Particles. Wiley-Interscience, New York
Bradley J.P., Brownlee D.E., 1991, Sci 251, 519
Brodsky M.H., Cardona M., Cuomo J.J., 1977, Phys. Rev. B 16, 3556
Canham L.T., 1990, Appl. Phys. Lett. 57, 1946
Cox P., Deharveng L., Caplan J., 1987, A&A 171, 277
Darbon S., Perrin J.-M., Sivan J.-P., 1998, A&A 333, 264
Darbon S., Zavagno A., Savine C., et al., 1999a, In: Cox P., Kessler M.F. (eds.) The Universe as seen by ISO. ESA SP-427, ESTEC, Noordwijk, The Netherlands, p. 667
Darbon S., Perrin J.-M., Sivan J.-P., 1999b, A&A 348, 990
Estes M.J., Moddel G., 1996a, Appl. Phys. Lett. 68, 1814
Estes M.J., Moddel G., 1996b, Phys. Rev. B 54, 14633
d'Hendecourt L., Léger A., Olofsson G., Schmidt W., 1986, A&A 170, 91
Frogel J.A., Persson S.E., 1972, ApJ 178, 667
Furton D.G., Witt A.N., 1992, ApJ 386, 587
Furton D.G., Witt A.N., 1993, ApJ 415, L51
Gordon K.D., Witt A.N., Friedmann B.C., 1998, ApJ 498, 522
Heydari-Malayeri M., Testor G., 1981, A&A 96, 229
Hofmeister H., Huiken F., Kohn B., 1999, Europ. Phys. S. D, in press
Hunter D.A., Massey P., 1990, AJ 99, 846
Kachurin G.A., Tyschenko I.E., Zhuravlev K.S., et al., 1997, Nucl. Instr. and Meth. in Phys. Res. B 122, 571
Kerr T.H., Hurst M.E., Miles J.R., Savre P.J., 1999, MNRAS 303, 446
Koshida N., Koyama H., Suda Y., et al., 1993, Appl. Phys. Lett. 63, 2774
Lamy P.L., Perrin J.-M., 1997, A&A 327, 1147
Landgraf M., Augustsson K., Grün E., Gustafson B.A.S., 1999, Sci 286, 2319
Ledoux G., Ehbrecht M., Guillois O., et al., 1998, A&A 333, L39
Ledoux G., 1999, Ph.D. Thesis, École doctorale des matériaux de Lyon
Léger A., Boissel P., d'Hendecourt L., 1988, Phys. Rev. Letter 60, 921

Lemaître G., Kohler D., Meunier J.-P., Vin A., 1990, A&A 228, 546
Lu Z.H., Lockwood D.J., Baribeau J.-M., 1995, Nat 378, 258
Nandy K., Thompson G.I., Jamar C., Monfils A., Wilson R., 1976, A&A 51, 63
Nash D.B., 1966, J. Geophys. Res. 71, 2517
Nash D.B., Matson D.L., Johnson T.V., Fanale F.P., 1975, J. Geophys. Res. 80, 1875
Noguchi N., Suemune I., Yamanischi M., Hua G.C., Otsuca N., 1992, Jpn. J. Appl. Phys. 31, 490
Papoular R., Conard J., Giuliano M., Kister J., Mille M., 1989, A&A 217, 204
Perrin J.-M., Sivan J.-P., 1992, A&A 255, 271
Perrin J.-M., Darbon S., Sivan J.-P., 1995, A&A 304, L21
Puget J.-L., Léger A., 1989, ARA&A 27, 161
Roelfsema P.R., Cox P., Kessler M.F., Baluteau J.-P., 1998, In: Yun J.L., Liseau R. (eds.) Star Formation With The Infrared Space Observatory (ISO). ASP Conf. Ser. 132, p. 76
Sakata A., Wada S., Narsawa T., et al., 1992, ApJ 393, L83
Schmidt G.D., Cohen M., Margon B., 1980, ApJ 239, L133
Seahra S., Duley W.W., 1999, ApJ 520, 719
Sellgren K., 1981, ApJ 245, 138
Sivan J.-P., Perrin J.-M., 1993, ApJ 404, 258
Szomoru A., Guhathakurta P., 1998, ApJ 494, L93
Theiß W., 1997, Surface Science Reports 29, 91
von Behren J., Üçer K.B., Tsybeskov L., Vandyshev Ju.V., Fauchet P.M., 1995, J. Vac. Sci. Technol. B13, 1225
Wilson W.L., Szajowski P.F., Bras L.E., 1993, Sci 262, 1242
Witt A.N., 1985, ApJ 216, 224
Witt A.N., Boroson T.A., 1990, ApJ 355, 182
Witt A.N., Gordon K.D., Furton D.G., 1998, ApJ 501, L111
Zavagno A., Ducci V., 1999, In: Cox P., Kessler M.F. (eds.) The Universe as seen by ISO. ESA SP-427, ESTEC, Noordwijk, The Netherlands, p. 791
Zubko V.O., Smith T.L., Witt A.N., 1999 ApJ 511, L57